Molecular Biology of the Cell
Vol. 12, 101–114, January 2001

# The Export of Major Histocompatibility Complex Class I Molecules from the Endoplasmic Reticulum of Rat Brown Adipose Cells Is Acutely Stimulated by Insulin

**Daniela Malide,*† Jonathan W. Yewdell,‡ Jack R. Bennink,‡ and Samuel W. Cushman***

*Experimental Diabetes, Metabolism, and Nutrition Section, Diabetes Branch, National Institute of Diabetes and Digestive and Kidney Diseases; and ‡Laboratory of Viral Diseases, National Institute of Allergy and Infectious Diseases, National Institutes of Health, Bethesda, Maryland 20892

Submitted January 19, 2000; Revised August 25, 2000; Accepted October 23, 2000
Monitoring Editor: Peter Walter

Major histocompatibility complex class I (MHC-I) molecules have been implicated in several nonimmunological functions including the regulation and intracellular trafficking of the insulin-responsive glucose transporter GLUT4. We have used confocal microscopy to compare the effects of insulin on the intracellular trafficking of MHC-I and GLUT4 in freshly isolated rat brown adipose cells. We also used a recombinant vaccinia virus (rVV) to express influenza virus hemagglutinin (HA) as a generic integral membrane glycoprotein to distinguish global versus specific enhancement of protein export from the endoplasmic reticulum (ER) in response to insulin. In the absence of insulin, MHC-I molecules largely colocalize with the ER-resident protein calnexin and remain distinct from intracellular pools of GLUT4. Surprisingly, insulin induces the rapid export of MHC-I molecules from the ER with a concomitant approximately three-fold increase in their level on the cell surface. This ER export is blocked by brefeldin A and wortmannin but is unaffected by cytochalasin D, indicating that insulin stimulates the rapid transport of MHC-I molecules from the ER to the plasma membrane via the Golgi complex in a phosphatidylinositol 3-kinase–dependent and actin-independent manner. We further show that the effect of insulin on MHC-I molecules is selective, because insulin does not affect the intracellular distribution or cell-surface localization of rVV-expressed HA. These results demonstrate that in rat brown adipose cells MHC-I molecule export from the ER is stimulated by insulin and provide the first evidence that the trafficking of MHC-I molecules is acutely regulated by a hormone.

## INTRODUCTION

Major histocompatibility complex class I molecules (MHC-I) consist of an integral membrane glycoprotein ($\alpha$-chain) noncovalently complexed to a small soluble chain ($\beta_2$-microglobulin). Vertebrates encode two types of MHC-I termed "classical" and "nonclassical." The present study concerns classical MHC-I, which function to bind peptides of 8–10 residues and present them at the cell surface to CD8+ T-cells, enabling immune surveillance of intracellular proteins (Heemels and Ploegh, 1995). This function is extensively documented and well characterized at the structural and cell biological levels (Yewdell and Bennink, 1992; Pamer and Cresswell, 1998).

Because of the expression of classical MHC-I in virtually all nucleated cells in vertebrates, numerous attempts have been made to demonstrate a nonimmunological function for these molecules, but so far none has been convincingly established (reviewed by Stagsted, 1998). Evidence from studies using coprecipitation assays and fluorescence energy transfer suggests a structural and functional association between MHC-I and insulin receptors (IR) (reviewed by Stagsted, 1998). In addition, MHC-I-derived peptides have been reported to inhibit internalization of some receptors such as IR and insulin-like growth factor (IGF)-I and IGF-II receptors, increasing their steady-state numbers on the cell surface and thereby enhancing the sensitivity to hormones and other agonists (Stagsted *et al.*, 1993a,b,c; Olsson *et al.*, 1994). Peptides derived from the $\alpha$1-region of MHC-I enhance

† Corresponding author and present address: Laboratory of Viral Diseases, National Institute of Allergy and Infectious Diseases, National Institutes of Health, Bethesda, MD 20892. E-mail address: dmalide@nih.gov.

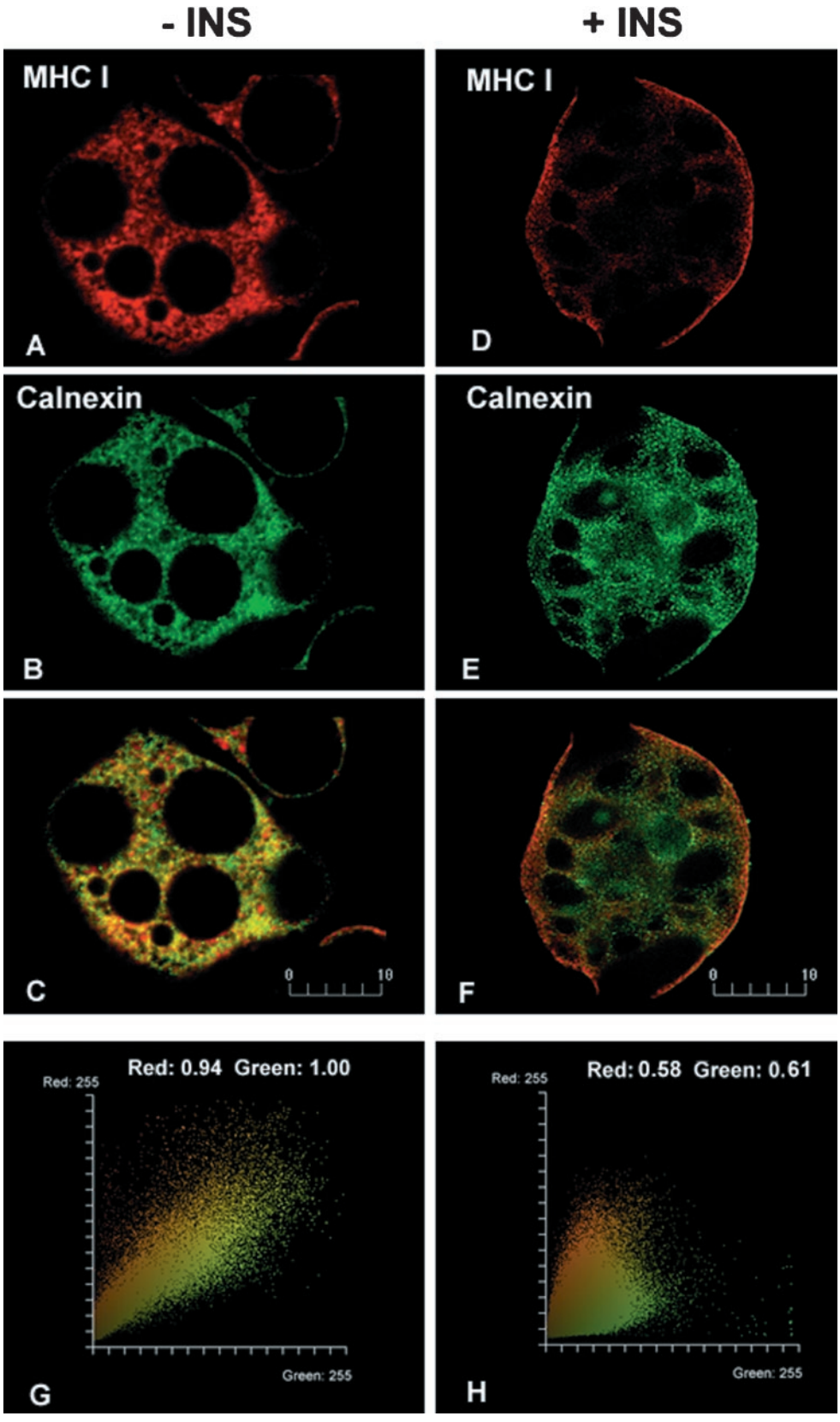
- INS
+ INS
MHC I
A
MHC I
D
Calnexin
B
Calnexin
E
0
10
C
0
10
F
Red: 0.94 Green: 1.00
Red: 255
Green: 255
G
Red: 0.58 Green: 0.61
Red: 255
Green: 255
H

glucose uptake in rat adipose cells above the maximum levels obtained with insulin stimulation alone because of inhibition of GLUT4 internalization (Stagsted *et al.*, 1990, 1993c). Collectively, these results suggest that MHC-I may be involved in the regulation and internalization of cell-surface integral membrane proteins such as GLUT4, IR, IGF-I receptors, and IGF-II receptors, based on the assumption that the effects of the peptides reflect either an inhibition or enhancement of normal MHC-I function.

If such a functional relationship exists between MHC-I and the internalization of various plasma membrane proteins, then MHC-I themselves may very well undergo subcellular trafficking, and this process might be regulated by the same receptors whose functions are influenced by MHC-I. To address this question, we have used rat brown adipose cells to assess the relationship between the MHC-I and GLUT4 compartments and their trafficking pathways. We have previously characterized the subcellular localization of GLUT4 and various organelle markers in these cells, which are physiological targets for insulin action (Malide *et al.*, 1997a). Using confocal microscopy and a novel method of quantitative image analysis, we provide evidence that the MHC-I and GLUT4 compartments are nonoverlapping in both unstimulated and insulin-stimulated cells, but that insulin exhibits a very surprising selective stimulation of the export of MHC-I from the endoplasmic reticulum (ER). This is the first report that the trafficking of MHC-I is acutely regulated by a hormone.

## MATERIALS AND METHODS

### *Preparation and Incubation of Adipose Cells*

Male Sprague Dawley rats (170–200 g, CD strain) from Charles River Breeding Laboratories (Boston, MA) were used. Brown adipose cells were isolated using collagenase digestion as described previously (Omatsu-Kanbe *et al.*, 1996). All incubations were carried out at 37°C in a Krebs-Ringer-bicarbonate-HEPES (KRBH) buffer, pH 7.4, containing 10 mM sodium bicarbonate, 30 mM HEPES, 200 nM adenosine, and 1% bovine serum albumin (fraction V) (BSA) from Intergen (Purchase, NY). Isolated adipose cells were incubated without (basal) or with (insulin-stimulated) 67 nM insulin (Eli Lilly, Indianapolis, IN) at 37°C for 30 min. The effects of wortmannin (WT), brefeldin A (BFA), and cytochalasin D (CytoD) (all from Sigma, St. Louis, MO) were also investigated. Thus, cells were incubated without or with 100 nM WT, 10–40 $\mu$g/ml BFA, or 10 $\mu$M CytoD for 30 min at 37°C before the addition of insulin for 30 min or 10 min after the addition of insulin for 30 min at 37°C in the continuous presence of insulin as previously described (Chakrabarti *et al.*, 1994; Malide and Cushman, 1997; Malide *et al.*, 1997b).

### *Antibodies*

The following antibodies and conjugates were from commercially available sources and have been previously characterized and used in immunofluorescence studies: the mouse monoclonal antibody OX-18 (10 $\mu$g/ml) anti-rat MHC class I antigen from Serotec-Harlan (Indianapolis, IN) and from Harlan Sera-Lab (Loughborough, United Kingdom) (Kaltschmidt *et al.*, 1995; Neumann *et al.*, 1995); a mouse monoclonal antibody MCA 1740 (5 $\mu$g/ml) anti-rat $\beta_2$-microglobulin from Serotec (Oxford, United Kingdom) (Flaris *et al.*, 1993); an affinity-purified rabbit polyclonal anti-GLUT4 antibody (0.15 $\mu$g/ml) recognizing a peptide of 20 amino acid residues from the C terminus of GLUT4, kindly provided by Hoffmann-La Roche (Nutley, NJ) (Malide *et al.*, 1997a); the anti-canine calnexin-C rabbit polyclonal antibody SPA-860 (1:100 dilution of whole serum) from Stressgen Biotechnologies Corp. (Victoria, British Columbia, Canada) (Chavez *et al.*, 1996; Barr *et al.*, 1997); phalloidin-rhodamine (1:200 dilution), used to localize F actin microfilaments, from Molecular Probes (Eugene, OR); and Texas Red-conjugated streptavidin (2 $\mu$g/ml) and fluorescein isothiocyanate- (FITC-), lissamine rhodamine sulfonyl chloride-, and Cy5-conjugated antibodies specific for rabbit or mouse immunoglobulins (Ig), used at 1:100 dilutions as secondary antibodies in immunofluorescence experiments, from Jackson ImmunoResearch (West Grove, PA). Additional Alexa 488- and Alexa 568-conjugated antibodies, used at 1:100 dilutions, were obtained from Molecular Probes. FITC- and biotin-conjugated antibodies specific for mouse isotypes (IgG1 and IgG2a), used as secondary antibodies in triple-labeling experiments, were obtained from PharMingen (San Diego, CA).

The following primary antibodies have been previously characterized: the mouse monoclonal antibodies Y8–10C2, H17-L2, and H28-E23 (neat ascites fluid) that recognize the monomeric and/or trimeric forms of the influenza virus hemagglutinin (HA) (Yewdell *et al.*, 1988); a mouse monoclonal anti-mannosidase II antibody (1:2 dilution of ascites fluid) (Burke *et al.*, 1982); and an affinity-purified rabbit polyclonal anti-clathrin heavy chain antibody (1:300) (Simpson *et al.*, 1996).

### *Expression of HA and an Enhanced Green Fluorescent Protein (EGFP)-tagged Influenza Virus Nucleoprotein (NP-EGFP) in Rat Adipose Cells using Recombinant Vaccinia Viruses (rVV)*

Brown adipose tissue was removed under sterile conditions, and the isolated cells were suspended in sterile KRBH buffer, pH 7.4, containing 5% BSA, 25 mM glucose, 25 mM HEPES, 4 mM L-glutamine, 200 nM (−)-$N^6$-(2-phenylisopropyl)-adenosine, and 75 $\mu$g/ml gentamicin to a cytocrit of 40% (5–6 $\times$ $10^6$ cells/ml). Aliquots (200 $\mu$l) of the cell suspension were dispensed into 1.0 ml of KRBH buffer in two chamber slides (Lab Tek 177429; Nunc, Naperville, IL). Cells were then infected with a rVV that encodes either HA or NP-EGFP for 5 h at 37°C, in a 5% $CO_2$ incubator, in the presence of 25 $\mu$g/ml cycloheximide and 25 $\mu$g/ml emetine (Sigma). The production and characterization of these rVVs have been described (Bennink *et al.*, 1984; Anton *et al.*, 1999). Five-hour postinfection samples corresponding to the cells from one chamber slide were distributed into 1.5-ml microcentrifuge tubes and washed four times in KRBH buffer, containing 5% BSA to remove free viruses. After incubation without or with insulin for 30 min at 37°C, intracellular trafficking was halted by quickly transferring the cells to ice and rinsing them with ice-cold phosphate-buffered saline (PBS) 0.15 M, pH 7.4. Sub-

**Figure 1.** Colocalization analysis of MHC-I and calnexin in basal (−INS; A–C) and insulin-stimulated (+INS; D–F) brown adipose cells. Without insulin, MHC-I (A) and calnexin (B) show very similar staining patterns. A high degree of colocalization is shown in yellow in the merged image (C) and in the quantitative analysis (G); the fluorogram depicts a diagonal-like distribution of dual-color pixels and high colocalization coefficients (red and green values ~1.0). In the presence of 67 nM insulin, MHC-I staining changes to a narrow peripheral rim (D), whereas the calnexin reticular staining remains unchanged (E). A merged image (F) and fluorogram (H) show a decreased colocalization of MHC-I and calnexin as depicted by a widely dispersed distribution of dual-color pixels and lower colocalization coefficients (values ~0.6). Bars, 10 $\mu$m. Images were obtained by imaging at least 10 cells for each experimental condition; all experiments were performed at least twice. The intensity of the fluorescence varied little from cell to cell.

sequently, cells were stained either without or with fixation and permeabilization as described below.

### *Indirect Immunofluorescence*

Isolated adipose cells were fixed in 2% paraformaldehyde (Electron Microscopy Sciences, Ft. Washington, PA) in 0.15 M PBS, pH 7.4, for 20 min at room temperature. In studies of the subcellular distributions of various proteins, cells were permeabilized, and single- and double-immunofluorescence experiments were performed as described (Malide *et al.*, 1997a). In triple-labeling experiments, cells were incubated simultaneously with all three of the primary antibodies overnight at 4°C, rinsed, and then incubated simultaneously with the isotype-specific secondary antibodies for 1 h at room temperature. A combination of FITC-labeled anti-mouse IgG1, biotinylated-anti-mouse IgG2a followed by streptavidin-Texas Red, and Cy5-labeled anti-rabbit IgG was used to detect the primary antibodies OX-18 (IgG1), H28E23 (IgG2a), and rabbit anti-GLUT4 IgG, respectively.

In addition, for comparative quantitative analysis of the fluorescence associated with only the cell surface, live brown adipose cells were stained unfixed and nonpermeabilized for MHC-I. Cells were rinsed quickly with ice-cold PBS and chilled to 4°C, then incubated with the anti-MHC-I (OX-18) antibodies in the absence of saponin for 30 min in an ice-water bath; cells were then washed, aldehyde fixed, incubated in the absence of saponin with fluorescently labeled goat anti-mouse IgG, washed again, and mounted in Vectashield (Vector Laboratories Inc, Burlingame, CA). Similarly, vaccinia-infected live cells were also stained for cell-surface expression of HA using both primary and secondary fluorescent labeled antibodies before aldehyde fixation.

### *Confocal Image Acquisition and Analysis*

Staining was observed with a Optiphot 2 fluorescence microscope (Nikon, Tokyo, Japan) equipped with an MRC-1024 confocal laser scanning microscope controlled by Lasersharp image acquisition and analysis software from Bio-Rad Laboratories (Hercules, CA). For each experimental condition, 10–15 cells were imaged separately by Kalman averaging 8–10 frames/image using a planapochromat 60X/1.4 NA oil objective at optical zooms between 1 and 2.5. The excitation wavelengths used were 488, 568, and 647-nm from a 15-mW krypton/argon laser. Sequential collection and 522DF32, 605DF32, 680DF32 bandpass emission filters were used to image the double- and triple-labeled cells separately to completely avoid cross-talk between the three emission signals. GFP was detected using an FITC setting. For three-dimensional reconstruction, series of optical sections were collected at 0.5-$\mu$m intervals along the *Z*-axis.

### *Quantitation of Fluorescence*

Z-series of high resolution images (512 × 512 pixels; 92 nm$^2$/pixel) were collected for whole cell-surface labeling and processed using Lasersharp 2.1 software. The "seed fill" algorithm of this software was applied to the three-dimensional series to extract individual cells based on pixel connectivity and a given range of intensity. Use of this algorithm was particularly advantageous because it provides a direct measurement of cell volume as well as the total number of interconnected voxels. The average background level was determined on a single optical section and used to set the black level of the intensity range. The upper limit of the 8-bit gray scale was set using the value of the most intense pixel in the region of interest. The resulting data were then used to calculate the integrated sum of total fluorescence through all optical sections in the three-dimensional series. This summation gave the total fluorescence per cell, and results were then compared among cells of similar size from different experimental conditions.

For illustration purposes, a two-dimensional projection (using the maximum-pixel intensity algorithm) of the three-dimensional seed-fill data was generated, and two-dimensional histogram plots of fluorescence intensities were obtained. Fluorescence intensities were color coded using a look-up table custom-designed to give maximum contrast to the total dynamic range of the images (0–40: dark blue; 41–75: medium blue; 76–100: light blue; 101–150: green; 151–215: red; 216–254: pink; 255: white). This look-up table was then applied to generate pseudocolor-mapped images. Images were acquired during the same day, typically from 10 cells of similar size from each experimental condition using identical settings of the instrument that avoided saturation of the brightest pixels. Similar results were obtained in three separate experiments. To analyze whether the change in fluorescence intensity was due to a change in the subcellular distribution, total cellular fluorescence was also determined on cells fixed and permeabilized before staining for MHC-I.

### *Colocalization Analysis*

Colocalization was assessed throughout the cell by examination of merged images. To quantitate the overlap of MHC-I and calnexin staining, colocalization was further analyzed using Lasersharp 3.1 software. Analysis was performed on only high resolution (512 × 512 pixels; 92 nm$^2$/pixel) single optical sections (not on projections). In addition to the merged image showing colocalized regions, a pixel fluorogram and two (red and green) colocalization coefficients were generated (as described in the Bio-Rad technical note 08/1998). The fluorogram is a two-dimensional intensity histogram of the dual-color image indicating the distribution of all pixels within the merged image as a scattergram, similar to the one used in flow cytometry. Pixel values of green and red components are displayed along the *x*- and *y*-axes, respectively. The colocalization coefficients are defined as the ratio of the integral of the intensity distribution of colocalizing objects and the total intensity of the respective components of the image. A high degree of colocalization is revealed by a diagonal distribution (at 45°) of the dots (pixels) on the fluorogram, and the colocalization coefficients are both almost equal to 1.0. A lack of colocalization is shown by two distinct populations (with minimal overlap) of dots (pixels) distributed toward the red and green axes, respectively, and the two colocalization coefficients both equal to zero (Manders *et al.*, 1993; Demandolx and Davoust, 1997; Amirand *et al.*, 1998). For presentation, digitized images were cropped and assembled using Adobe Photoshop 5.0 software from Adobe Systems (Mountain View, CA) and printed with a Kodak 8650 PS digital printer (Eastman Kodak, New Haven, CT).

## RESULTS

### *Insulin Induces a Rapid Export of MHC-I from the ER to the Cell Surface*

To address the question whether MHC-I share a common subcellular trafficking pathway with insulin-regulated GLUT4, we studied the localization and fate of these molecules in brown adipose cells. We used confocal microscopy and a novel technique for quantitative image analysis to examine staining with a monoclonal antibody specific for a polymorphic determinant on rat class I molecules. In isolated brown adipose cells in the absence of insulin, few MHC-I are detected on the cell surface; the majority of the MHC-I is distributed intracellularly, located in a reticular, honeycombed pattern throughout the cytoplasm (Figure 1A). Unexpectedly, brief incubation (30 min) with insulin results in a rapid redistribution of MHC-I to the cell surface (Figure 1D). Similar findings were made using an anti-$\beta_2$-microglobulin antibody, making it rather unlikely that we

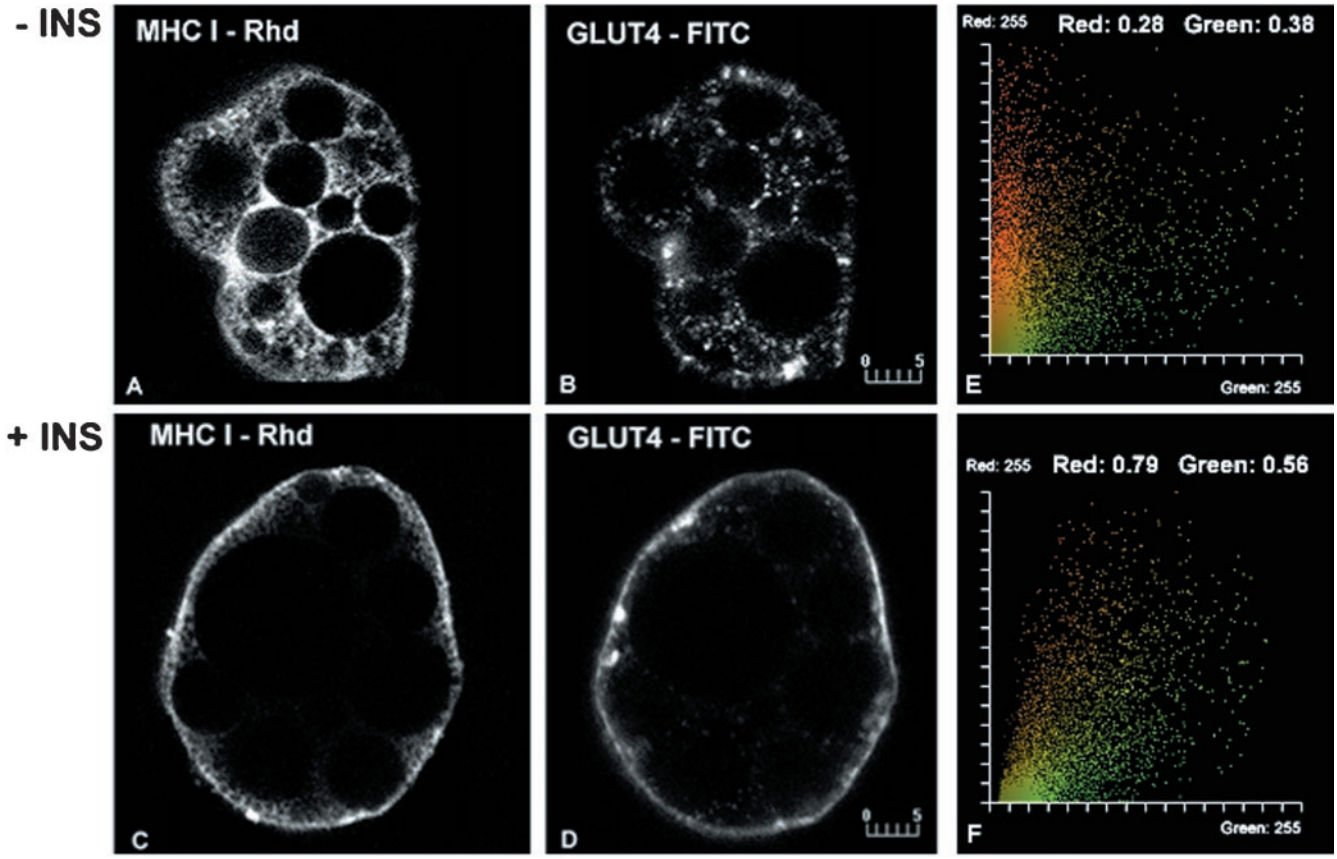


**Figure 2.** Colocalization analysis of MHC-I and GLUT4 in basal (−INS; A and B) and insulin-stimulated (+INS; C and D) brown adipose cells. Without insulin, MHC-I (A) and GLUT4 (B) show completely distinct reticular and punctate patterns, respectively. Consistent with the visual appearance, the fluorogram (E) shows little overlap and low colocalization coefficients (values ~0.3). In the presence of 67 nM insulin, both MHC-I (C) and GLUT4 (D) display staining which outlines the cell periphery. An increased degree of colocalization of MHC-I and GLUT4 in this region is shown in the fluorogram (F) and by the corresponding colocalization coefficients (values ~0.8 and 0.6, respectively). Bars, 5 $\mu$m.

were detecting an unrelated molecule that cross-reacted with the antibodies. The basal pattern of MHC-I staining resembles that of the ER in adipose cells (Barr *et al.*, 1997). Indeed, double-labeling of cells not exposed to insulin demonstrates nearly complete colocalization of MHC-I and the ER-resident protein calnexin (Figure 1, A–C). After exposure to insulin, calnexin remains in the ER and MHC-I are largely exported to the plasma membrane (Figure 1, D–F).

To support these data, we performed quantitative analysis of the colocalization of these two molecules (Figure 1, G and H). Consistent with the visual impression, the fluorograms illustrate narrow, diagonal-like, distributions of dual-color pixels in the absence of insulin (Figure 1G) and much more widely dispersed distributions in the presence of insulin (Figure 1H). The colocalization coefficients show MHC-I values close to 1.0 in the absence of insulin and ~ 0.6 in the presence of insulin in the particular optical section shown. Similar analyses were performed on optical sections collected throughout the cell, which confirm that, in the presence of insulin, the proportion of MHC-I colocalized with calnexin decreases from 100 to 40%. We have tried to confirm the ER localization of MHC-I using immunoelectron microscopy on cryosections of brown adipose tissue. Our attempts in this direction have so far been unsuccessful, probably because of the relatively low level of MHC-I.

### *MHC-I and GLUT4 Localize to Distinct Intracellular Compartments*

The remarkable effect of insulin on MHC-I subcellular distribution prompted us to compare the localization of MHC-I with GLUT4 in brown adipose cells. In the absence of insulin, GLUT4 is present in a punctate distribution distinct from the reticular distribution of MHC-I (Figure 2, A and B). Quantitative analysis of the staining reveals low values for the colocalization coefficients (Figure 2E). In the presence of insulin, both proteins display a rim of immunofluorescence at the cell surface (Figure 2, C and D) and increased colocalization (Figure 2F).

### *BFA Blocks the Export of MHC-I from the ER but Does Not Inhibit GLUT4 Translocation from a Post-Golgi Compartment to the Cell Surface*

The redistribution of GLUT4 to the cell surface in response to insulin is known to occur through a vesicle translocation

mechanism (Cushman and Wardzala, 1980; Suzuki and Kono, 1980). Given the nearly exclusive ER localization of MHC-I and the insulin-induced depletion of this compartment, it appeared likely that cell-surface class I molecules were recruited from the ER. We tested this hypothesis by stimulating adipose cells with insulin in the presence of BFA, which blocks export of proteins from the ER-Golgi complex intermediate compartment in a variety of cell types (Klausner *et al.*, 1992). Because the effects of BFA have not been well characterized in rat brown adipose cells, we first established that BFA redistributes the medial Golgi complex protein mannosidase II and the trans-Golgi network-associated clathrin as demonstrated in other cells. However, ~10-fold greater amounts of BFA are required (35–40 $\mu$g/ml), and the effects require ~10-fold more time (30 min) compared with other cells, probably because of the high lipid content of these cells and the lipophilic properties of the drug.

Preincubation of rat adipose cells with BFA before insulin prevents the appearance of MHC-I on the cell surface, resulting in MHC-I staining that is comparable to that seen in basal cells (Figure 3A). In contrast, the insulin-stimulated translocation of GLUT4 to the cell surface is not prevented by BFA, although GLUT4 occasionally appear in tubular structures (Figure 3B). These data show that the MHC-I, but not the GLUT4, pathway to the cell surface has BFA-sensitive step(s), most likely at the level of export from the ER-Golgi intermediate compartment.

Because BFA affects endosomal and trans-Golgi network morphology differentially, we attempted to use BFA to dissect the recycling pathway(s) from the cell surface to the inside of the cell in the presence of insulin. Cells were preincubated with insulin for 10 min, followed by BFA in the continuous presence of insulin for an additional 30 min. Under these conditions, most of the MHC-I and GLUT4 is detected at the cell surface (Figure 3, C and D), with some GLUT4, but not MHC-I, now present in structures resembling the tubular transferrin receptor-containing endosomes seen after BFA treatment in other cell types (Figure 3, E and F). These findings indicate that, although the trafficking of both MHC-I and GLUT4 is influenced by insulin, distinct mechanisms are used.

### *WT Inhibits Both MHC-I Export from the ER and GLUT4 Translocation*

To further characterize the trafficking pathways for MHC-I, we investigated the effects of WT in brown adipose cells. WT has been shown to block GLUT4 exocytosis by primarily inhibiting insulin signaling at the phosphatidyl-inositol 3-kinase level. WT also induces vacuolization of the endosomal system by preventing early-endosomal autoantigen-Rab5–mediated attachment to membranes (Simonsen *et al.*, 1998; Christoforidis *et al.*, 1999). Preincubation of cells with WT before insulin completely blocks the insulin-stimulated redistribution of MHC-I and GLUT4 to the cell surface (Figure 4, A and B). However, if cells are preincubated with insulin, WT does not decrease MHC-I associated with the cell surface as it does GLUT4; nor is it associated with the appearance of MHC-I in enlarged vacuolar structures as previously described for GLUT4 (Figure 4, C and D).

### *Actin-independent Exocytosis of MHC-I and GLUT4 in Response to Insulin*

Previous studies indicate that the actin network plays a role in the stimulatory action of insulin on glucose transport (Tsakiridis *et al.*, 1997; Wang *et al.*, 1998). Actin has also been implicated in the trafficking of MHC-I in HeLa cells (Radhakrishna and Donaldson, 1997). To examine the role of actin in MHC-I trafficking in insulin-stimulated rat adipose cells, we incubated cells with CytoD, which disassembles the actin network. Actin disassembly does not prevent the insulin-induced movement of either MHC-I or GLUT4 to the cell surface (Figure 5, A and B). Moreover, when cells are preincubated with insulin, CytoD does not decrease the cell-surface distribution of MHC-I, although it markedly redistributes peripheral GLUT4 into ring-like structures (Figure 5, C and D), providing further evidence for the differential trafficking of MHC-I and GLUT4. The effect of CytoD on actin microfilaments was verified by staining with rhodamine-phalloidin (Figure 5, E and F).

### *Quantitative Analysis of MHC-I on the Surface of Living Cells*

Cell fixation and permeabilization can bias antigen quantitation by differentially affecting molecules present in different locales. To quantitate more accurately the relative numbers of MHC-I present at the cell surface, we stained live brown adipose cells. Under the conditions used, no fluorescent signal was detectable intracellularly, demonstrating the integrity of the plasma membrane. The results are illustrated in Figure 6, A–D, where, for visualization purposes, two-dimensional projections of the data have been generated and color coded to reveal the dynamic range in fluorescence values. The corresponding two-dimensional histogram plots of fluorescence intensities are also depicted (Figure 6, bottom). Insulin stimulation results in a three-fold increase in cell-surface MHC-I. This is markedly decreased by preincubation with BFA and completely inhibited by preincubation with WT. To confirm that the change in fluorescence intensity is due to a change in the subcellular distribution, total cellular fluorescence was also determined on cells fixed and permeabilized before staining for MHC-I. Under these conditions, similar values of total fluorescence are obtained in cells incubated in the absence and presence of insulin.

### *Insulin Does Not Affect the Subcellular Localization of rVV-Expressed HA*

A crucial issue is whether insulin specifically mobilizes MHC-I from the ER or has a general effect on the trafficking of integral membrane proteins assembled in the ER. We investigated this question using rVVs as vectors to express cell-surface integral membrane proteins. VV has been used to express proteins in a wide variety of cells, but its ability to infect freshly isolated adipose cells has not been reported (Wyatt *et al.*, 1995; Olson *et al.*, 1997). Infection of rat adipose cells using an rVV encoding NP-EGFP results in detectable expression in ~90% of the cells 5 h postinfection. VV infection does not interfere with the insulin-induced redistribution of either MHC-I or GLUT4 (Figure 7).

We next examined the effect of insulin on the trafficking of VV-encoded influenza virus HA. The export of HA from the

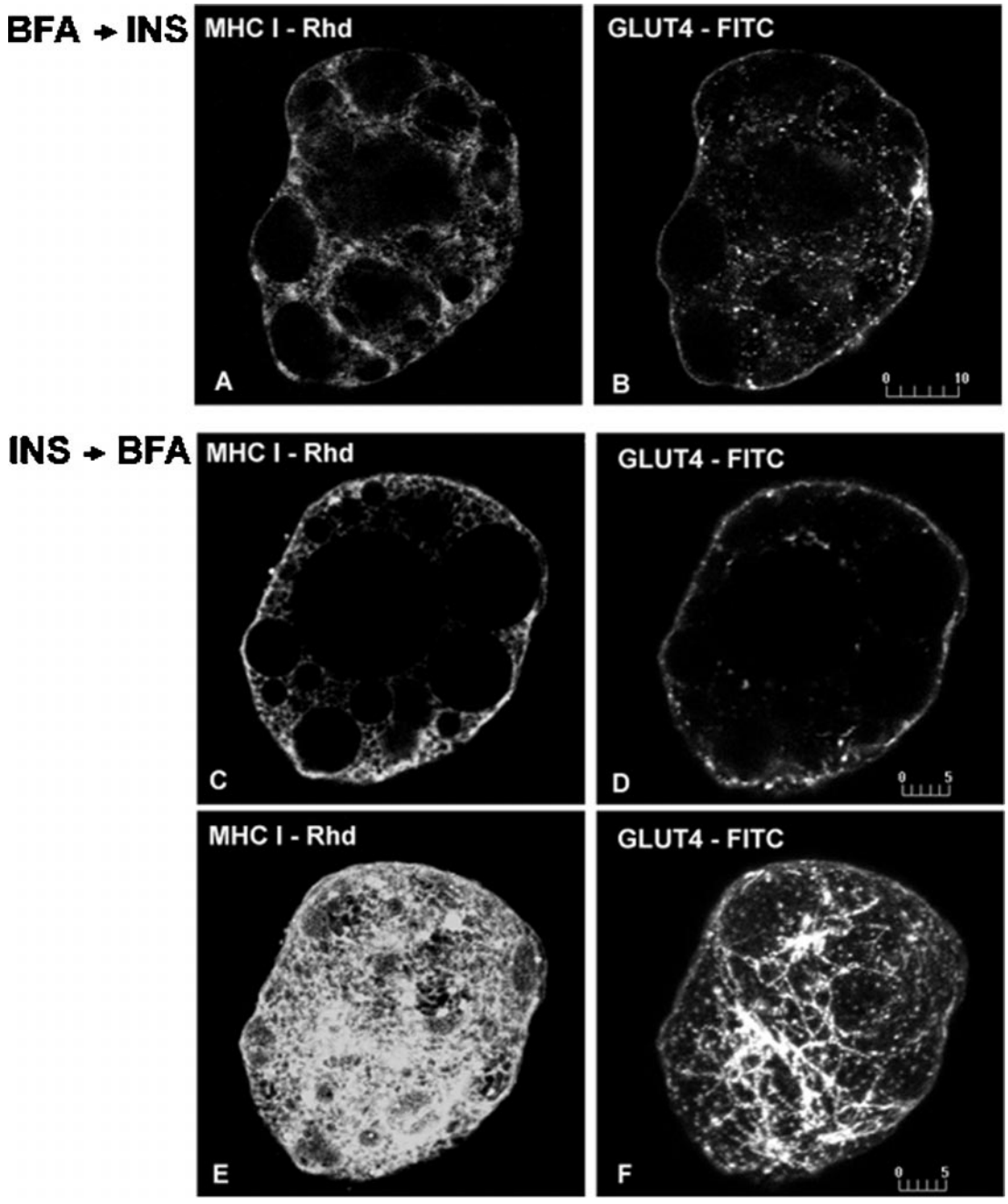


**Figure 3.** Dual immunofluorescence of MHC-I and GLUT4 in brown adipose cells incubated with BFA before (A and B) and after (C–F) insulin treatment. In cells incubated for 30 min with 35 $\mu$g/ml BFA, followed by 30 min with 67 nM insulin, MHC-I show a reticular, basal-like distribution and no detectable staining on the cell surface (A). In contrast, GLUT4 continue to exhibit a cell-surface pattern outlining the cell periphery (B). When cells are first incubated for 10 min with insulin, followed for 30 min with BFA in the continuous presence of insulin, most of the MHC-I (C) and GLUT4 (D) staining remains in a peripheral rim pattern in single optical sections. In addition, GLUT4 (F) but not MHC-I (E) display tubule-like staining clearly visible in whole cell images. E and F represent projections of 15 optical sections. Bars, 10 $\mu$m (A and B); 5 $\mu$m (C–F).

ER to the cell surface has been characterized in many cell types (Roth *et al.*, 1989). In addition, the availability of antibodies distinguishing between the monomeric form of the protein found in the ER and the trimeric form localized to the secretory pathway make HA an ideal marker of the constitutive exocytic pathway (Russ *et al.*, 1991). When expressed in basal cells, the majority of HA localizes intracellularly in a reticular pattern, similar to that of MHC-I and

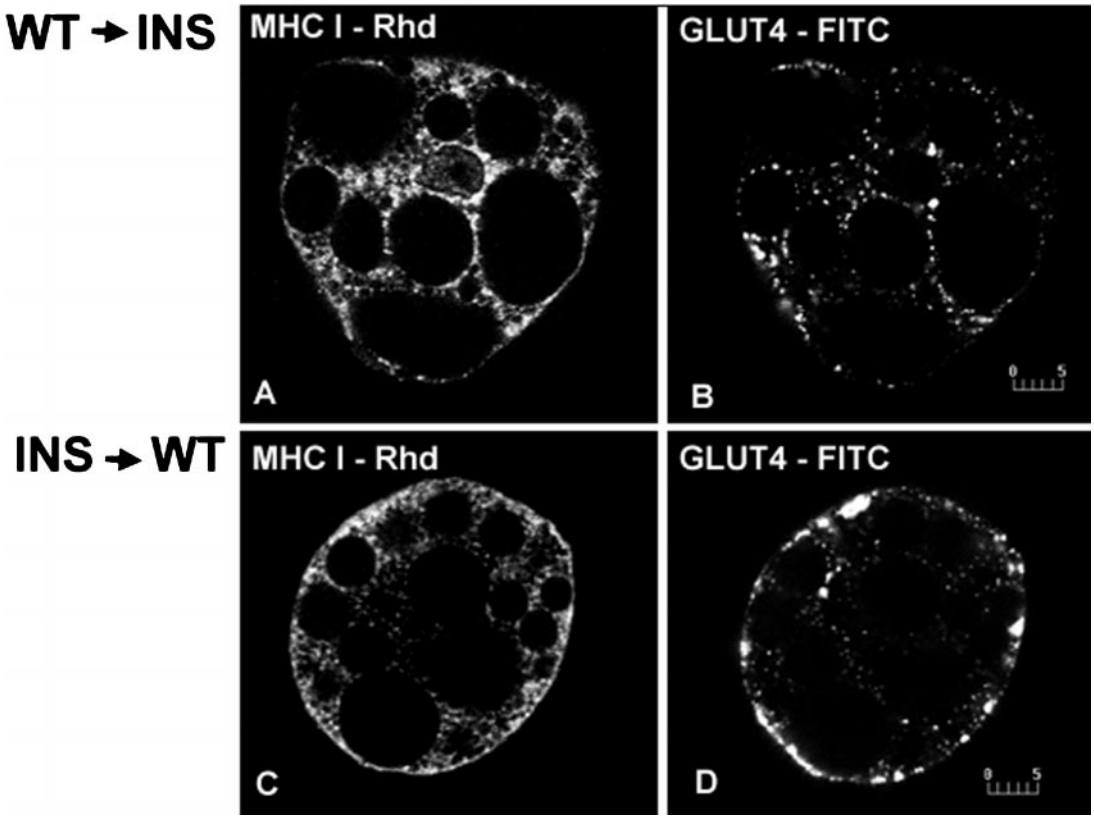


**Figure 4.** Simultaneous localization of MHC-I and GLUT4 in brown adipose cells incubated with WT before (A and B) and after (C and D) insulin (INS) treatment. In cells incubated with 100 nM WT before 67 nM insulin, MHC-I (A) and GLUT4 (B) exhibit only intracellular reticular and punctate staining, respectively, comparable to the basal patterns. When cells are preincubated with insulin, WT does not decrease MHC-I staining, which outlines the cell surface (C), but redistributes most of the cell-surface GLUT4 staining into a vacuole-like pattern (D). Bars, 5 $\mu$m.

clearly distinct from GLUT4 (Figure 8, A–C). Relatively low amounts of HA are detected on the surface of live cells (Figure 8G). After cells are exposed to insulin, much of the HA remains intracellular and reticular, in marked contrast to the redistribution of both MHC-I and GLUT4 to the cell surface (Figure 8, D–F). In addition, the cell-surface-associated HA immunofluorescence in living cells is not quantitatively altered in response to insulin (Figure 8H). These findings indicate that insulin exerts a selective effect on mobilizing MHC-I release from the ER.

## DISCUSSION

In this study we provide clear evidence that, in the absence of insulin stimulation, MHC-I and GLUT4 are localized to distinct, nonoverlapping subcellular compartments in rat brown adipose cells. MHC-I are present in the ER, whereas GLUT4 exist in a post-ER compartment. Unexpectedly, insulin induces the export of MHC-I from the ER with a concomitant approximately three-fold increase in cell-surface MHC-I. This process is blocked by WT and BFA but is actin independent. Insulin-modulated control of MHC-I export from the ER represents the first instance in which either MHC-I or the highly-related MHC-II have been shown to be under hormonal control. Importantly, insulin does not affect the intracellular distribution and cell-surface localization of rVV-expressed HA, indicating that the insulin-induced export of MHC-I from the ER is selective.

The extent to which hormonal control of MHC-I exocytosis applies to other cell types remains to be established. Although textbooks routinely state that MHC-I are expressed on nearly all cell types, the dynamic control of MHC-I in differentiated non-bone-marrow–derived cells has not been examined. Although the functional ramifications of hormonal control of antigen presentation remain to be established experimentally, it is not difficult to imagine how this could impact normal immune responses or autoimmune responses to self-antigens or how endocrinological diseases, particularly diabetes mellitus, might interfere with normal hormonal regulation.

The mechanism by which insulin selectively induces the rapid export of MHC-I from the ER is unclear. The current understanding of MHC-I biogenesis is that newly assembled $\alpha$–$\beta_2$-microglobulin heterodimers are retained in the ER until they acquire high-affinity peptides, whose binding induces a conformational alteration that releases the heterodimers from dedicated or general ER-retained chaperones. Because MHC-I that lack high-affinity peptides

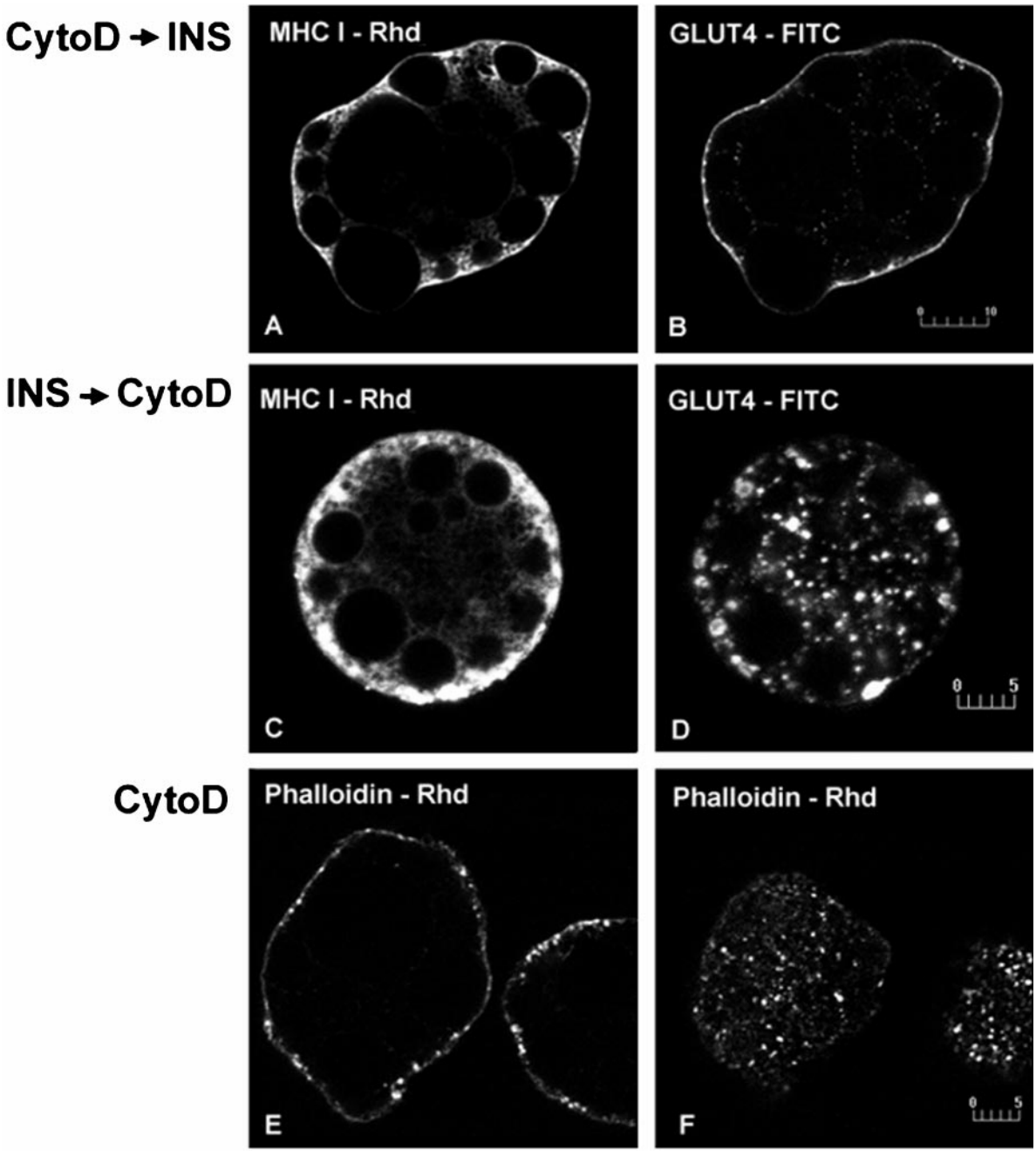


**Figure 5.** Simultaneous localization of MHC-I and GLUT4 in brown adipose cells incubated with CytoD before (A and B) and after (C and D) insulin (INS) treatment. In cells incubated for 30 min with 10 $\mu$M CytoD followed by 30 min with 67 nM insulin, MHC-I (A) and GLUT4 (B) show cell-surface staining outlining the cell periphery. In cells incubated first for 10 min with insulin, followed by 30 min with CytoD in the continuous presence of insulin, MHC-I (C) cell-surface staining does not decrease, whereas GLUT4 (D) markedly redistributes to ring-like peripheral structures. In CytoD-treated cells, F-actin labeled using phalloidin-rhodamine show punctate staining, indicating actin disassembly (E and F). Bars, 10 $\mu$m (A and B); 5 $\mu$m (C–F).

denature rapidly on the cell surface, releasing $\beta_2$-microglobulin to the surrounding medium, the observation that $\beta_2$-microglobulin remains on the cell surface upon insulin stimulation argues that the MHC-I released from the ER bear peptides of typical affinity. It seems likely, therefore, that the retention of MHC-I is based on a specific interaction of completed molecules with a novel ligand and that insulin stimulation modifies the ligand to release MHC-I. This ER-export is blocked by WT, indicating a PI3-kinase–dependent process. The signal remains to be established but might

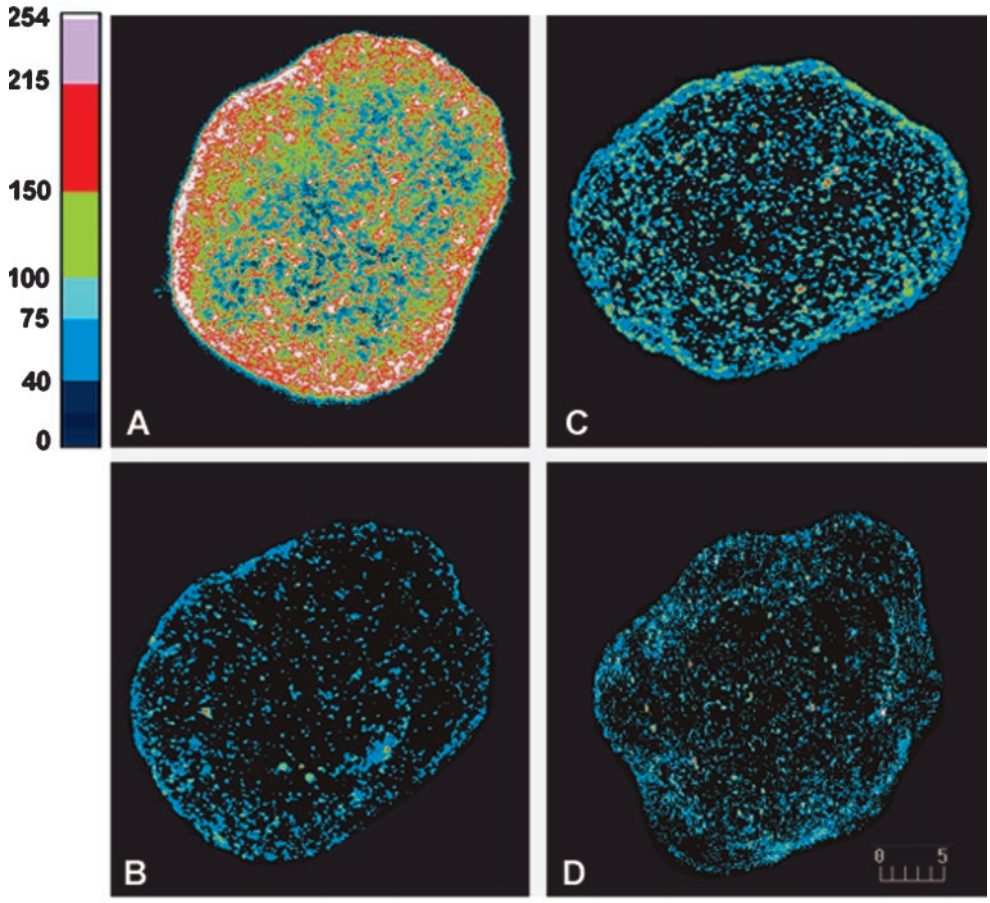


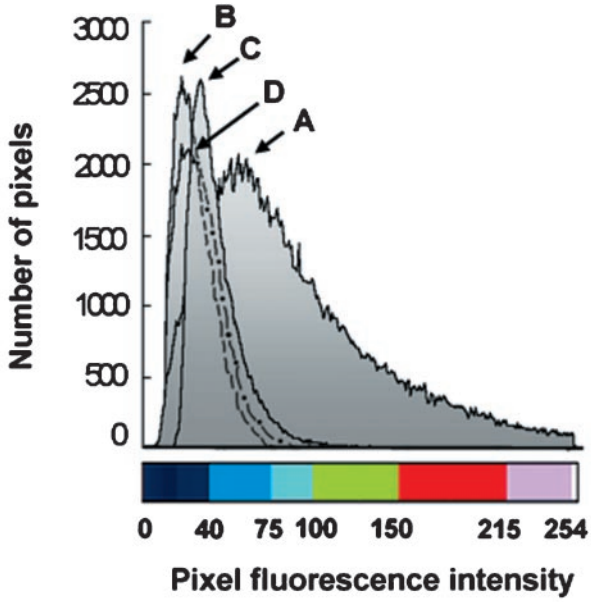


**Figure 6.** Quantitative analysis of cell-surface MHC-I immunofluorescence in brown adipose cells. Cells were incubated with (A) or without 67 nM insulin (B) and with 35 $\mu$g/ml BFA (C) and 100 nM WT (D) before insulin treatment; living cells were stained for cell-surface MHC-I, and whole-cell fluorescence was calculated using Lasersharp 2.1 software as described in MATERIALS AND METHODS. For illustration purposes, two-dimensional projections of the three-dimensional data were generated and pseudocolor mapped using a look-up table (top four images); two-dimensional histogram plots of the fluorescence intensities were compiled (bottom). MHC-I fluorescence intensity increases three-fold in cells incubated with insulin (A, image and corresponding histogram plot) compared with control cells (B); preincubation with BFA (C) and WT (D) prevents the insulin-induced enhancement of cell-surface MHC-I. Bar, 5 $\mu$m. Quantitative analysis was performed on five size-matched cells for each experimental condition, and experiments were performed three times.

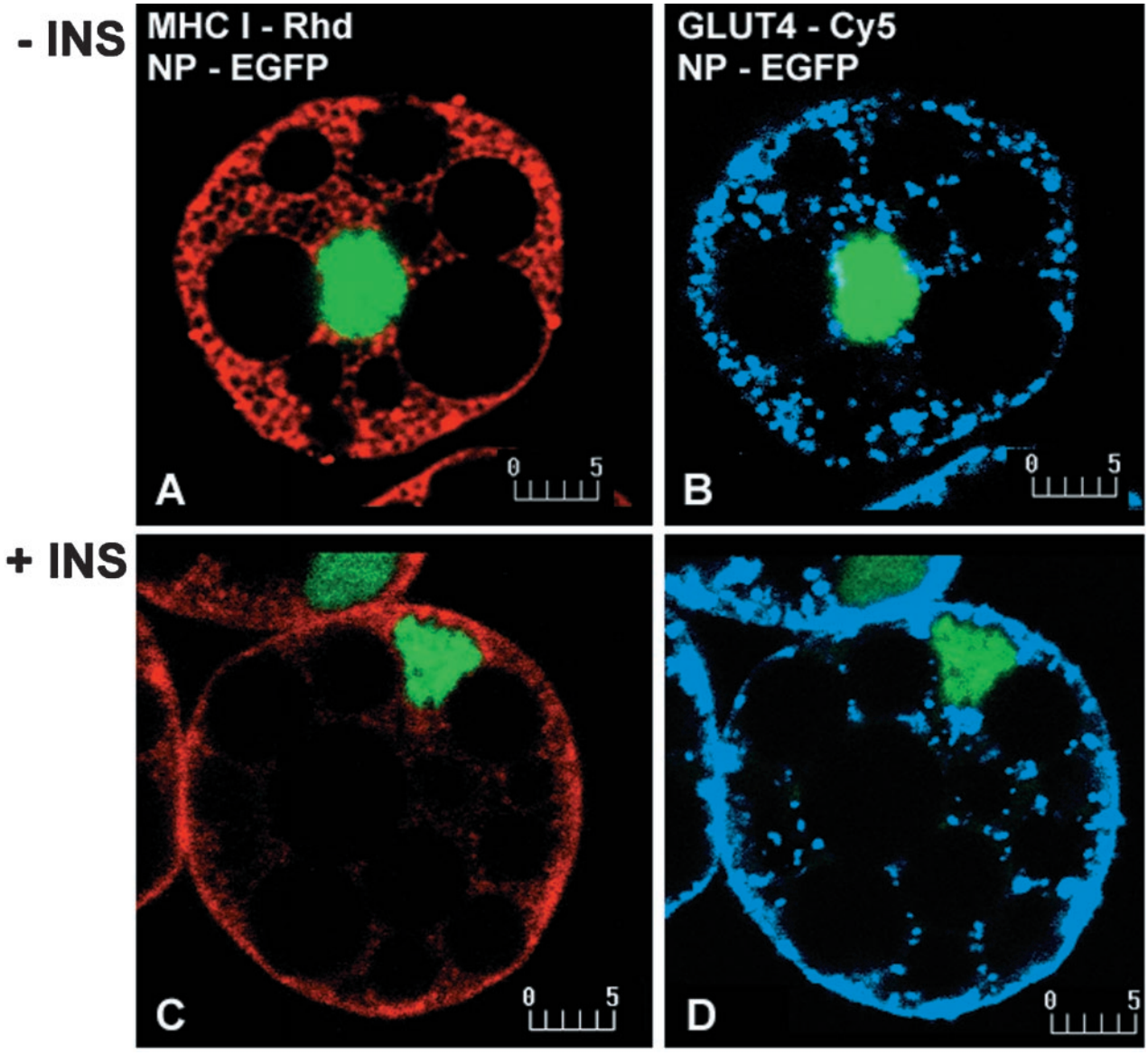


**Figure 7.** Localization of MHC-I and GLUT4 in basal (−INS; A and B) and insulin-stimulated (+INS; C and D) brown adipose cells expressing NP-EGFP using an rVV. NP-EGFP was transiently expressed using an rVV. Infected cells were then incubated in the absence and presence of 67 nM insulin for 30 min, fixed, and immunofluorescently stained for endogenous MHC-I and GLUT4. NP-EGFP was visualized directly, and MHC-I and GLUT4 were detected using Rhd- and Cy5-labeled secondary antibodies, respectively. In basal cells, MHC-I (A) and GLUT4 (B) show the characteristic reticular and punctate patterns, respectively; in insulin-treated cells, both MHC-I (C) and GLUT4 (D) show outlining peripheral rim staining comparable to the patterns seen in noninfected cells. Bars, 5 $\mu$m.

involve the recruitment of the p85 subunit of PI3-kinase to the ER, as suggested by our preliminary data. The released molecules then follow a route through the Golgi, as inhibited by BFA, to the cell surface.

We used immunofluorescence quantitative analysis, and MHC-I and GLUT4 appear to localize at distinct microdomains of the plasma membrane. Further characterization of this difference will require immunoelectron microscopy. Our attempts in this direction have so far been unsuccessful, probably because of the relatively low level of MHC-I. Previous studies using fluorescence resonance energy transfer and immunogold electron microscopy revealed a nonrandom, clustered distribution pattern of MHC-I in human T and B lymphoid cell lines (Bodnar *et al.*, 1996; Jenei *et al.*, 1997). Modification of membrane cholesterol levels affects expression and clustering of MHC-I in cells of the immune system (Bodnar *et al.*, 1996), and it will be of interest to determine whether MHC-I exhibits an association with specialized membrane lipid domains in adipose cells. In these cells ~13% of the plasma membrane consists of morphologically recognizable caveolae (Goldberg *et al.*, 1987; Scherer *et al.*, 1994). These presumably play an important functional

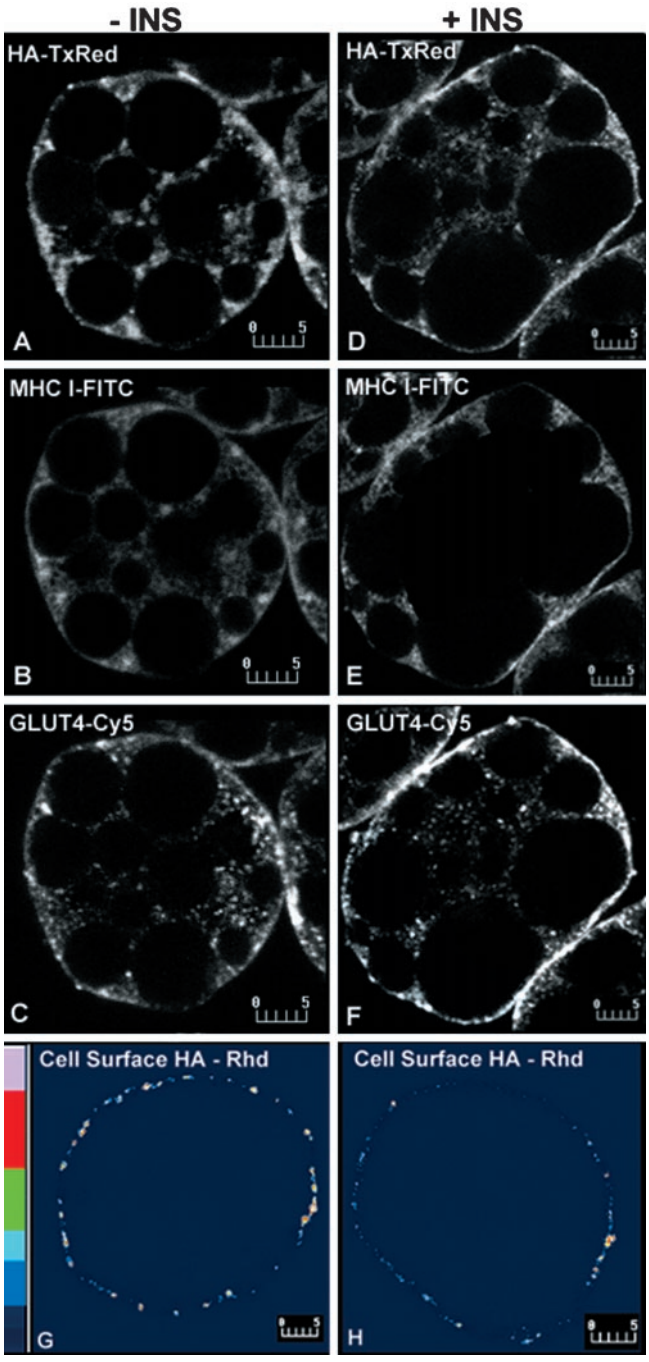


**Figure 8.** Simultaneous localization of MHC-I-, GLUT4-, and rVV-expressed HA in basal (−INS; A–C) and insulin-stimulated (+INS; D–F) brown adipose cells. Influenza virus HA was transiently expressed using the rVV system. Infected cells were incubated in the absence or presence of 67 nM insulin for 30 min and then processed for confocal microscopy. For triple labeling using fixed and permeabilized cells, HA was detected using biotinylated isotype-specific secondary antibodies and Texas Red-conjugated streptavidin; MHC-I, using FITC-conjugated isotype-specific secondary antibodies; and GLUT4 using Cy5-conjugated secondary antibodies. In basal cells, HA (A) shows a reticular pattern similar to that of MHC-I (B) and clearly distinct from the punctate GLUT4 pattern (C). In insulin-treated cells, HA (D) staining remains largely unchanged, in marked contrast to the redistribution of both MHC-I (E) and GLUT4 (F) to a peripheral rim. Cell-surface immunofluorescence of HA expressed in living cells remains quantitatively unchanged in response to insulin (H) compared with basal cells (G); (~3.5 and ~4.2 arbitrary units in the 1–255 scale). Bars, 5 $\mu$m.

role in signal transduction, which has yet to be characterized. Inasmuch as MHC-I are integral membrane proteins (and not glycosyl-phosphatidylinositol anchored), they are unlikely to be localized to caveolae, leaving the differential distribution of MHC-I and GLUT4 a completely open question.

The insulin-induced movement of MHC-I to the cell surface in adipose cells appears to be a one-way process. Thus, in marked contrast to GLUT4, which continuously recycle between the cell surface and a post-Golgi complex compartment and can be seen in vacuolized endosomes as induced by WT and tubular endosomes as induced by BFA, the distribution of MHC-I is unaffected under the same conditions. MHC-I have been reported to be spontaneously internalized in some cells and even to recycle (Machy *et al.*, 1987a,b; Stang *et al.*, 1997). However, this has not been observed in most cell lines tested (Neefjes *et al.*, 1990; Glickman *et al.*, 1996), and our findings suggest that class I molecules do not constitutively recycle in either resting or insulin-stimulated brown adipose cells.

The question of whether insulin-stimulated GLUT4 exocytosis occurs through a regulated secretory pathway has been difficult to address. Morphological and kinetic data argue that GLUT4 and either leptin or adipsin share the same transport vesicles after insulin treatment (Kitagawa *et al.*, 1989; Calderhead *et al.*, 1990; Barr *et al.*, 1997). Furthermore, insulin-induced GLUT4 exocytosis is insensitive to BFA, consistent with the localization of GLUT4 to a post-Golgi compartment. However, like MHC-I exocytosis, GLUT4 translocation to the cell surface is dependent on PI3-kinase but not on actin microfilaments as disassembled by CytoD. Together with our previous evidence on leptin secretion, these results demonstrate that adipose cells exhibit at least two distinct processes of insulin-stimulated exocytosis: the first consists of MHC-I export and leptin secretion from the ER; the second comprises GLUT4 translocation from a post-Golgi compartment. The former is also consistent with a very recent report of insulin-stimulated secretion of the adipocyte complement-related protein of 30 kDa (ACRP30) from 3T3-L1 adipocytes (Bogan and Lodish, 1999).

In contrast to MHC-I, GLUT4 internalize from the surface of the cells. Our current results show that treatment of adipose cells with insulin followed by BFA induces the appearance of GLUT4 in tubular, endosome-like structures but without a change in the insulin-stimulated level of GLUT4 on the cell surface. These data are similar to previous observations of a morphological redistribution of GLUT4, together with several recycling receptors such as transferrin receptor, to tubule-like structures in cultured muscle cells incubated with BFA without insulin (Ralston and Ploug, 1996). These findings further support the concept that the GLUT4 endocytic pathway shares some common steps with the endocytosis of membrane receptors. However, our GLUT4 data suggest that recycling continues unaltered in

the presence of BFA, despite the profound morphological changes. It also appears that GLUT4 trafficking from the plasma membrane in the presence of insulin occurs through actin-dependent steps; this is indicated by a reorganization of peripheral GLUT4 from a cell-surface rim to ring-like structures in response to treatment first with insulin followed by actin disassembly. It remains to be established whether these ring-like structures are part of or separate from the plasma membrane.

Finally, we have shown for the first time that rVV can be used as a transient expression system in freshly isolated brown adipose cells. Our results demonstrate high infection efficiency in a time frame that allows protein detection by immunofluorescence at a relatively short time interval after virus infection. Importantly, we show that the production of proteins under the control of early viral promoters does not compromise the insulin response. In parallel experiments, we observed that rVV are equally adept at expressing proteins in white adipose cells. As an efficient means of transiently expressing proteins in a high percentage of cells, rVV should prove to be a valuable tool for both morphological and biochemical analyses of adipose cells.

## ACKNOWLEDGMENTS

We thank Steven R. Richards for technical assistance. We thank Samuel A. Tesfai, Bio-Rad Laboratories, for his advice and many helpful discussions on the quantitative analysis of immunofluorescence. We thank Drs. J. Paul Luzio, Barbara R. Reaves, and Maragaret S. Robinson (Cambridge University, UK) for generously providing the anti-mannosidase II and anti-clathrin heavy chain antibodies, respectively. D.M. is particularly indebted to Dr. Jan W. Slot and all members of Dr. Hans J. Geuze's laboratory (Department of Cell Biology, University of Utrecht, The Netherlands), for their instruction in the technique of ultrathin cryo-sectioning, and for their example and inspiration in its use, and to Dr. Lennart Olsson (Receptron Inc., Mountain View, CA) for supporting this training. We thank Drs. Ian A. Simpson and Evelyn Ralston for continuous help and encouragement and for critically reading the manuscript.

## REFERENCES

Amirand, C., Viari, A., Ballini, J.P., Rezaei, H., Beaujean, N., Jullien, D., Kas, E., and Debey, P. (1998). Three distinct sub-nuclear populations of HMG-I protein of different properties revealed by colocalization image analysis. J. Cell Sci. *111*, 3551–3561.

Anton, L.C., Schubert, U., Bacik, I., Princiotta, M.F., Wearsch, P.A., Gibbs, J., Day, P.M., Realini, C., Rechsteiner, M.C., Bennink, J.R., and Yewdell, J.W. (1999). Intracellular localization of proteasomal degradation of a viral antigen. J. Cell Biol. *146*, 113–124.

Barr, V.A., Malide, D., Zarnowski, M.J., Taylor, S.I., and Cushman, S.W. (1997). Insulin stimulates both leptin secretion and production by rat white adipose tissue. Endocrinology *138*, 4463–4472.

Bennink, J.R., Yewdell, J.W., Smith, G.L., Moller, C., and Moss, B. (1984). Recombinant vaccinia virus primes and stimulates influenza hemagglutinin-specific cytotoxic T cells. Nature *311*, 578–579.

Bodnar, A., Jenei, A., Bene, L., Damjanovich, S., and Matko, J. (1996). Modification of membrane cholesterol level affects expression and clustering of class I HLA molecules at the surface of JY human lymphoblasts. Immunol. Lett. *54*, 221–226.

Bogan, J.S., and Lodish, H.F. (1999). Two compartments for insulin-stimulated exocytosis in 3T3–L1 adipocytes defined by endogenous ACRP30 and GLUT4. J. Cell Biol. *146*, 609–620.

Burke, B., Griffiths, G., Reggio, H., Louvard, D., and Warren, G. (1982). A monoclonal antibody against a 135-K Golgi membrane protein. EMBO J. *1*, 1621–1628.

Calderhead, D.M., Kitagawa, K., Tanner, L.I., Holman, G.D., and Lienhard, G.E. (1990). Insulin regulation of the two glucose transporters in 3T3–L1 adipocytes. J. Biol. Chem. *265*, 13801–13808.

Chakrabarti, R., Buxton, J., Joly, M., and Corvera, S. (1994). Insulin-sensitive association of GLUT-4 with endocytic clathrin-coated vesicles revealed with the use of brefeldin A. J. Biol. Chem. *269*, 7926–7933.

Chavez, R.A., Miller, S.G., and Moore, H.P. (1996). A biosynthetic regulated secretory pathway in constitutive secretory cells. J. Cell Biol. *133*, 1177–1191.

Christoforidis, S., McBride, H.M., Burgoyne, R.D., and Zerial, M. (1999). The Rab5 effector EEA1 is a core component of endosome docking. Nature *397*, 621–625.

Cushman, S.W., and Wardzala, L.J. (1980). Potential mechanism of insulin action on glucose transport in the isolated rat adipose cell: apparent translocation of intracellular transport systems to the plasma membrane. J. Biol. Chem. *255*, 4758–4762.

Demandolx, D., and Davoust, J. (1997). Multicolor analysis and local image correlation in confocal microscopy. J. Microsc. *185*, 21–36.

Flaris, N.A., Densmore, T.L., Molleston, M.C., and Hickey, W.F. (1993). Characterization of microglia and macrophages in the central nervous system of rats: definition of the differential expression of molecules using standard and novel monoclonal antibodies in normal CNS and in four models of parenchymal reaction. Glia *7*, 34–40.

Glickman, J.N., Morton, P.A., Slot, J.W., Kornfeld, S., and Geuze, H.J. (1996). The biogenesis of the MHC class II compartment in human I-cell disease B lymphoblasts. J. Cell Biol. *132*, 769–785.

Goldberg, R.I., Smith, R.M., and Jarett, L. (1987). Insulin and alpha 2-macroglobulin-methylamine undergo endocytosis by different mechanisms in rat adipocytes: I. Comparison of cell surface events. J. Cell. Physiol. *133*, 203–212.

Heemels, M.T., and Ploegh, H. (1995). Generation, translocation, and presentation of MHC class I-restricted peptides. Annu. Rev. Biochem. *64*, 463–491.

Jenei, A., Varga, S., Bene, L., Matyus, L., Bodnar, A., Bacso, Z., Pieri, C., Gaspar, R., Farkas, T., and Damjanovich, S. (1997). HLA class I and II antigens are partially co-clustered in the plasma membrane of human lymphoblastoid cells. Proc. Natl. Acad. Sci. USA *94*, 7269–7274.

Kaltschmidt, C., Kaltschmidt, B., and Baeuerle, P.A. (1995). Stimulation of ionotropic glutamate receptors activates transcription factor NF-kappa B in primary neurons. Proc. Natl. Acad. Sci. USA *92*, 9618–9622.

Kitagawa, K., Rosen, B.S., Spiegelman, B.M., Lienhard, G.E., and Tanner, L.I. (1989). Insulin stimulates the acute release of adipsin from 3T3–L1 adipocytes. Biochim. Biophys. Acta *1014*, 83–89.

Klausner, R.D., Donaldson, J.G., and Lippincott-Schwartz, J. (1992). Brefeldin A: insights into the control of membrane traffic and organelle structure. J. Cell Biol. *116*, 1071–1080.

Machy, P., Truneh, A., Gennaro, D., and Hoffstein, S. (1987a). Endocytosis and de novo expression of major histocompatibility complex encoded class I molecules: kinetic and ultrastructural studies. Eur. J. Cell. Biol. *45*, 126–136.

Machy, P., Truneh, A., Gennaro, D., and Hoffstein, S. (1987b). Major histocompatibility complex class-I molecules internalized via coated pits in lymphocytes-T. Nature *328*, 724–726.

Malide, D., and Cushman, S.W. (1997). Morphological effects of wortmannin on the endosomal system and GLUT4-containing compartments in rat adipose cells. J. Cell Sci. *110*, 2795–2806.

Malide, D., Dwyer, N.K., Blanchette-Mackie, E.J., and Cushman, S.W. (1997a). Immunocytochemical evidence that GLUT4 resides in a specialized translocation post-endosomal VAMP2-positive compartment in rat adipose cells in the absence of insulin. J. Histochem. Cytochem. *45*, 1083–1096.

Malide, D., St-Denis, J.F., Keller, S.R., and Cushman, S.W. (1997b). Vp165 and GLUT4 share similar vesicle pools along their trafficking pathways in rat adipose cells. FEBS Lett. *409*, 461–468.

Manders, E.M.M., Verbeek, F.J., and Aten, J.A. (1993). Measurements of colocalizatiom of objects in dual-color confocal images. J. Microsc. *169*, 375–382.

Neefjes, J.J., Stollorz, V., Peters, P.J., Geuze, H.J., and Ploegh, H.L. (1990). The biosynthetic pathway of MHC class II but not class I molecules intersects the endocytic route. Cell *61*, 171–183.

Neumann, H., Cavalie, A., Jenne, D.E., and Wekerle, H. (1995). Induction of MHC class I genes in neurons. Science *269*, 549–552.

Olson, A.L., Knight, J.B., and Pessin, J.E. (1997). Syntaxin 4, VAMP2, and/or VAMP3/cellubrevin are functional target membrane and vesicle SNAP receptors for insulin-stimulated GLUT4 translocation in adipocytes. Mol. Cell. Biol. *17*, 2425–2435.

Olsson, L., Goldstein, A., and Stagsted, J. (1994). Regulation of receptor internalization by the major histocompatibility complex class I molecule. Proc. Natl. Acad. Sci. USA *91*, 9086–9090.

Omatsu-Kanbe, M., Zarnowski, M.J., and Cushman, S.W. (1996). Hormonal regulation of glucose transport in a brown adipose cell preparation isolated from rats that shows a large response to insulin. Biochem. J. *315*, 25–31.

Pamer, E., and Cresswell, P. (1998). Mechanisms of MHC class I-restricted antigen processing. Annu. Rev. Immunol. *16*, 323–358.

Radhakrishna, H., and Donaldson, J.G. (1997). ADP-ribosylation factor 6 regulates a novel plasma membrane recycling pathway. J. Cell Biol. *139*, 49–61.

Ralston, E., and Ploug, T. (1996). GLUT4 in cultured skeletal myotubes is segregated from the transferrin receptor and stored in vesicles associated with TGN. J. Cell Sci. *109*, 2967–2978.

Roth, M.G., Gething, M.J., and Sambrook, J. (1989). Membrane insertion and intracellular transport of influenza virus glycoproteins. In: The Influenza Viruses, ed. R.T. Krug, New York: Plenum Press, 219–267.

Russ, G., Bennink, J.R., Bachi, T., and Yewdell, J.W. (1991). Influenza virus hemagglutinin trimers and monomers maintain distinct biochemical modifications and intracellular distribution in brefeldin A-treated cells. Cell Regul. *2*, 549–563.

Scherer, P.E., Lisanti, M.P., Baldini, G., Sargiacomo, M., Mastick, C.C., and Lodish, H.F. (1994). Induction of caveolin during adipogenesis and association of GLUT4 with caveolin-rich vesicles. J. Cell Biol. *127*, 1233–1243.

Simonsen, A., Lippe, R., Christoforidis, S., Gaullier, J.M., Brech, A., Callaghan, J., Toh, B.H., Murphy, C., Zerial, M., and Stenmark, H. (1998). EEA1 links PI(3)K function to Rab5 regulation of endosome fusion. Nature *394*, 494–498.

Simpson, F., Bright, N.A., West, M.A., Newman, L.S., Darnell, R.B., and Robinson, M.S. (1996). A novel adaptor-related protein complex. J. Cell Biol. *133*, 749–760.

Stagsted, J. (1998). Journey beyond immunology: regulation of receptor internalization by major histocompatibility complex class I (MHC-I) and effect of peptides derived from MHC-I. APMIS Suppl. *85*, 1–40.

Stagsted, J., Mapelli, C., Meyers, C., Matthews, B.W., Anfinsen, C.B., Goldstein, A., and Olsson, L. (1993a). Amino acid residues essential for biological activity of a peptide derived from a major histocompatibility complex class I antigen. Proc. Natl. Acad. Sci. USA *90*, 7686–7690.

Stagsted, J., Olsson, L., Holman, G.D., Cushman, S.W., and Satoh, S. (1993b). Inhibition of internalization of glucose transporters and IGF-II receptors: mechanism of action of MHC class I-derived peptides which augment the insulin response in rat adipose cells. J. Biol. Chem. *268*, 22809–22813.

Stagsted, J., Reaven, G.M., Hansen, T., Goldstein, A., and Olsson, L. (1990). Regulation of insulin receptor functions by a peptide derived from a major histocompatibility complex class I antigen. Cell *62*, 297–307.

Stagsted, J., Ziebe, S., Satoh, S., Holman, G.D., Cushman, S.W., and Olsson, L. (1993c). Insulinomimetic effect on glucose transport by epidermal growth factor when combined with a major histocompatibility complex class I-derived peptide. J. Biol. Chem. *268*, 1770–1774.

Stang, E., Kartenbeck, J., and Parton, R.G. (1997). Major histocompatibility complex class I molecules mediate association of SV40 with caveolae. Mol. Biol. Cell *8*, 47–57.

Suzuki, K., and Kono, T. (1980). Evidence that insulin causes translocation of glucose transport activity to the plasma membrane from an intracellular storage site. Proc. Natl. Acad. Sci. USA *77*, 2542–2545.

Tsakiridis, T., Wang, Q., Taha, C., Grinstein, S., Downey, G., and Klip, A. (1997). Involvement of the actin network in insulin signaling. Soc. Gen. Physiol. Ser. *52*, 257–271.

Wang, Q., Bilan, P.J., Tsakiridis, T., Hinek, A., and Klip, A. (1998). Actin filaments participate in the relocalization of phosphatidylinositol 3-kinase to glucose transporter-containing compartments and in the stimulation of glucose uptake in 3T3–L1 adipocytes. Biochem. J. *331*, 917–928.

Wyatt, L.S., Moss, B., and Rozenblatt, S. (1995). Replication-deficient vaccinia virus encoding bacteriophage T7 RNA polymerase for transient gene expression in mammalian cells. Virology *210*, 202–205.

Yewdell, J.W., and Bennink, J.R. (1992). Cell biology of antigen processing and presentation to major histocompatibility complex class I molecule-restricted T lymphocytes. Adv. Immunol. *52*, 1–123.

Yewdell, J.W., Yellen, A., and Bachi, T. (1988). Monoclonal antibodies localize events in the folding, assembly, and intracellular transport of the influenza virus hemagglutinin glycoprotein. Cell *52*, 843–852.